Chin. J. Chem. Eng., **15**(5) 619—625 (2007)

Stability of Stratified Gas-Liquid Flow in Horizontal and Near Horizontal Pipes*

GU Hanyang(顾汉洋)[a,b,**] **and GUO Liejin**(郭烈锦)[a]
[a] State Key Laboratory of Multiphase Flow, Xi'an Jiaotong University, Xi'an 710049, China
[b] School of Nuclear Science and Engineering, Shanghai Jiao Tong University, Shanghai 200240, China

Abstract A viscous Kelvin-Helmholtz criterion of the interfacial wave instability is proposed in this paper based on the linear stability analysis of a transient one-dimensional two-fluid model. In this model, the pressure is evaluated using the local momentum balance rather than the hydrostatic approximation. The criterion predicts well the stability limit of stratified flow in horizontal and nearly horizontal pipes. The experimental and theoretical investigation on the effect of pipe inclination on the interfacial instability are carried out. It is found that the critical liquid height at the onset of interfacial wave instability is insensitive to the pipe inclination. However, the pipe inclination significantly affects critical superficial liquid velocity and wave velocity especially for low gas velocities.
Keywords two-fluid model, Kelvin-Helmholtz criterion, interfacial instability, gas-liquid stratified flow

1 INTRODUCTION

Stratified two-phase flow is one of the most commonly observed flow patterns in chemical industry and hence has been of continuing interest from both the practical and theoretical points of view[1—5]. Many pipeline systems are designed to operate in the stratified flow regime due to the lower pressure gradient and to avoid intermittent behavior. In horizontal and nearly horizontal pipes, the onset of interfacial wave instability for a gas-liquid stratified flow is usually related to the stratified-slug flow regime transition[6—9]. For most practical situations, the occurrence of slugs in pipes leads to negative effects. Therefore, it is important to study the instability of gas-liquid stratified flow for the design and operation of pipeline systems.

Considerable progress has been made in theoretical study of the instability of stratified flow. The classical inviscid Kelvin-Helmholtz instability analysis for gas-liquid interface in a horizontal rectangular pipe was first performed by Milne-Thomson[10] and Yih[11]. However, Wallis and Dobson[12] found that the critical liquid velocity predicted by the classical inviscid K-H instability analysis was about twice the experimental data. Taitel and Duckler[13] extended the K-H analysis to the case of a finite wave on a flat liquid sheet in horizontal channel flow and then to finite waves on stratified liquid in an inclined pipe, in which the criterion was also derived from the inviscid fluid theory.

Lin and Hanratty[14], Barnea[15], Barnea and Taitel[16] presented viscous K-H analysis using one-dimensional averaged two-fluid models. In their models, the effects of viscosity were introduced in through empirical walls and interfacial friction correlations. Compared to the experimental data, viscous analysis provided more accurate results than the inviscid analysis[7]. But all these authors neglected the normal component of viscous stress. Recently, Funada and Joseph[17] proved that the effect of normal stress was always important and played a role in determining the stability limits when the volume fraction of gas was not too small.

In this study, a new two-fluid model is developed to describe stratified flow in horizontal and near horizontal pipes, in which the effect of normal stress in each phase is taken into account. The criterion of onset of interfacial wave instability is derived based on linear analysis of the model. Then the characteristics of the interfacial wave of stratified flow in the horizontal and near horizontal pipes are investigated experimentally and compared to the criterion derived in this paper.

2 ONE-DIMENSIONAL TWO-FLUID MODEL

2.1 Governing equations

The one-dimensional transient two-fluid model is formulated by considering each phase in terms of cross section averaged governing equations of the balance of mass and momentum of each phase in the inclined pipe (Fig.1) as follows[15]:

Continuity equation:

$$\frac{\partial\left(A_l\rho_l\right)}{\partial t}+\frac{\partial\left(A_l\rho_l U_l\right)}{\partial x}=0 \qquad (1)$$

$$\frac{\partial\left(A_{\rm g}\rho_{\rm g}\right)}{\partial t}+\frac{\partial\left(A_{\rm g}\rho_{\rm g} U_{\rm g}\right)}{\partial x}=0 \qquad (2)$$

Momentum equation:

$$\frac{\partial\left(A_l\rho_l U_l\right)}{\partial t}+\frac{\partial\left(A_l\rho_l U_l^2\right)}{\partial x}= -\frac{\partial\left(A_l\rho_l\right)}{\partial x}+p_{{\rm i}l}\frac{\partial A_l}{\partial x}+\tau_{\rm i}S_{\rm i}-\tau_l S_{\rm l}-A_l\rho_l g\sin\theta \qquad (3)$$

Received 2006-12-20, accepted 2007-05-05.
* Supported by the National Natural Science Foundation of China (No.50521604) and Shanghai Jiao Tong University Young Teacher Foundation.
** To whom correspondence should be addressed. E-mail: guhanyang@sjtu.edu.cn

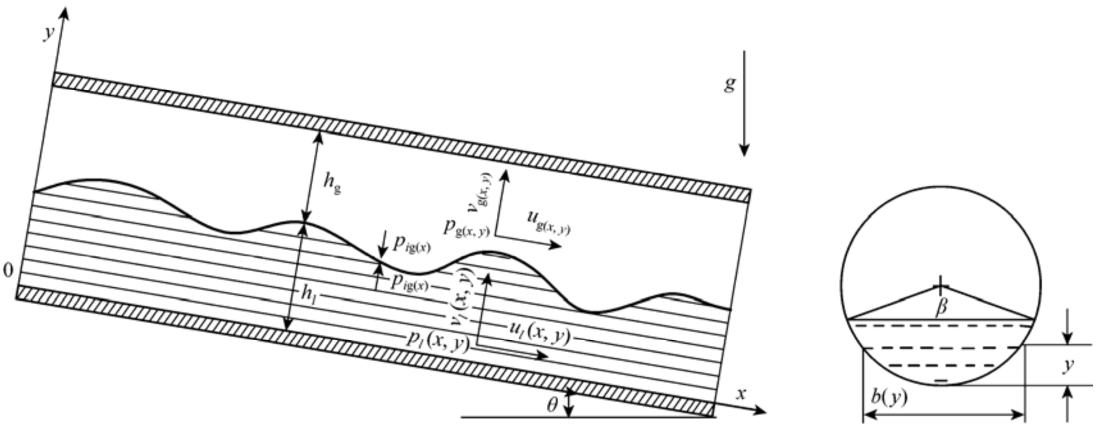

Figure 1 Gas-liquid stratified flow in a circular pipe

$$\frac{\partial\left(A_{\rm g}\rho_{\rm g}U_{\rm g}\right)}{\partial t}+\frac{\partial\left(A_{\rm g}\rho_{\rm g}U_{\rm g}^2\right)}{\partial x}=-\frac{\partial\left(A_{\rm g}P_{\rm g}\right)}{\partial x}+p_{\rm ig}\frac{\partial A_{\rm g}}{\partial x}-\tau_{\rm i}S_{\rm i}-\tau_{\rm g}S_{\rm g}-A_{\rm g}\rho_{\rm g}g\sin\theta \quad (4)$$

Here, each phase is assumed to be incompressible, and the heat and mass transfer between the two phases is ignored.

2.2 Closure relation

Former researchers obtained the following relations by adopting hydrostatic approximation[13—16] and neglecting the transverse component of the phase velocity:

$$p_l\left(y\right)=p_{{\rm i}l}+\rho_l g\cos\theta\left(h_l-y\right)$$
$$p_{\rm g}\left(y\right)=p_{\rm ig}+\rho_{\rm g}g\cos\theta\left(h_l-y\right) \quad (5)$$

However, Funada and Joseph[16] and Liu[18] found that the variance of the transverse component of the phase velocity played an important role in the interfacial wave propagation and development. In the following, a closure relation with the transverse component of phase velocities taken into account is deduced.

Starting with the definition of the cross-averaged pressure:

$$A_lP_l=\int_0^{h_l}p_l\left(y\right)b\left(y\right){\rm d}y \quad (6)$$

and introducing $p_l(y)$ as

$$p_l\left(y\right)=p_{{\rm i}l}+p_l'\left(y\right) \quad (7)$$

the needed pressure term can be expressed as a function of $p_l(y)$ using the Leibniz rule of derivation:

$$-\frac{\partial\left(A_lP_l\right)}{\partial x}+p_{{\rm i}l}\frac{\partial A_l}{\partial x}=-A_l\frac{\partial P_{{\rm i}l}}{\partial x}-\int_0^{h_l}\frac{\partial}{\partial x}p_0'\left(y\right)b\left(y\right){\rm d}y \quad (8)$$

Then modeling of $p_l'(y)$ in the right side of Eq.(8) has to be done next. Using the local momentum balance in the y-direction:

$$p_l\left[\frac{\partial v_l}{\partial t}+u_l\frac{\partial v_l}{\partial x}+v_l\frac{\partial v_l}{\partial y}\right]=-\frac{\partial p_l}{\partial y}-\rho_l g\cos\theta+\frac{\partial\tau_{xy}}{\partial x}+\frac{\partial\tau_{yy}}{\partial y} \quad (9)$$

So pressure $p_l'(y)$ can be expressed by

$$p_l'\left(y\right)\rho_l g\cos\theta\left(h_l-y\right)+\rho_l\int_y^{h_l}\varphi\left(x,y'\right){\rm d}y' \quad (10)$$

with

$$\varphi\left(x,y\right)=\frac{\partial v_l}{\partial t}+u_l\frac{\partial v_l}{\partial x}+v_l\frac{\partial v_l}{\partial y}-\mu_l\left(\frac{\partial^2u_l}{\partial x\partial y}+\frac{\partial^2v_l}{\partial x^2}+2\frac{\partial^2v_l}{\partial y^2}\right) \quad (11)$$

Then using Leibniz rule yields:

$$\int_0^{h_l}\frac{\partial}{\partial x}p_l'\left(y\right)b\left(y\right){\rm d}y=\underbrace{\rho_l\int_0^{h_l}g\cos\theta\frac{\partial h_l}{\partial x}b\left(y\right){\rm d}y}_{I_1}+\underbrace{\rho_l\int_0^{h_l}\varphi\left(x,h_l\right)\frac{\partial h_l}{\partial x}b\left(y\right){\rm d}y}_{I_2}+\underbrace{\rho_l\int_0^{h_l}\left[\int_y^{h_l}\frac{\partial}{\partial x}\varphi\left(x,y'\right){\rm d}y'\right]b\left(y\right){\rm d}y}_{I_3} \quad (12)$$

I_1 is easily obtained by integration as

$$I_1=\rho_lA_lg\cos\theta\frac{\partial h_l}{\partial x} \quad (13)$$

which is the hydrostatic term. The other two terms in the right side of Eq.(12) contain the contribution of the transient transverse acceleration. Following the approximations presented by the Barnerjee[19] leads to (Appendix A)

$$I_2=\rho_lA_l\frac{\partial h_l}{\partial x}\left[\frac{\partial}{\partial t}+U_l\left(x,h_l\right)\frac{\partial}{\partial x}\right]^2\left(h_l\right) \quad (14)$$

$$I_3=-\rho_lh_l^2A_l\eta\left[\frac{\partial}{\partial t}+U_l\frac{\partial}{\partial x}-\frac{\partial U_l}{\partial x}-\mu_l\frac{\partial^2}{\partial x^2}\right]\left(\frac{\partial^2}{\partial x^2}U_l\right) \quad (15)$$

with

$$\eta=\frac{1}{2}\left[1-\frac{1}{\pi}\frac{A}{A_l}\sin\left(\frac{\pi h_l}{4R}\right)\right].$$

So the following momentum equation for the liquid phase is obtained:

$$\frac{\partial\left(A_l\rho_l U_l\right)}{\partial t}+\frac{\partial\left(A_l\rho_l U_l^2\right)}{\partial x}=$$

$$-A_l\frac{\partial p_{il}}{\partial x}-I_1-I_2-I_3+\tau_i S_i-\tau_l S_l-A_l\rho_l g\sin\theta \quad (16a)$$

$$I_1=\rho_l A_l g\cos\theta\frac{\partial h_l}{\partial x} \quad (16b)$$

$$I_2=\rho_l A_l\frac{\partial h_l}{\partial x}\left[\frac{\partial}{\partial t}+U_l\left(x,h_l\right)\frac{\partial}{\partial x}\right]^2\left(h_l\right) \quad (16c)$$

$$I_3=-\rho_1 h_l^2 A_l\eta\left[\frac{\partial}{\partial t}+U_l\frac{\partial}{\partial x}-\frac{\partial U_l}{\partial x}-\mu_l\frac{\partial^2}{\partial x^2}\right]\left(\frac{\partial^2}{\partial x^2}U_l\right) \quad (16d)$$

$$\eta=\frac{1}{2}\left[1-\frac{1}{\pi}\frac{A}{A_l}\sin\left(\frac{\pi h_l}{4R}\right)\right] \quad (16e)$$

Similarly, the following momentum equations for the gas phase is obtained:

$$\frac{\partial\left(A_g\rho_g U_g\right)}{\partial t}+\frac{\partial\left(A_g\rho_g U_l^2\right)}{\partial x}=-A_g\frac{\partial p_{ig}}{\partial x}-$$

$$J_1-J_2-J_3-\tau_i S_i-\tau_g S_g-A_g\rho_g g\sin\theta \quad (17a)$$

$$J_1=\rho_g A_g g\cos\theta\frac{\partial h_l}{\partial x} \quad (17b)$$

$$J_2=\rho_g A_g\frac{\partial h_l}{\partial x}\left[\frac{\partial}{\partial t}+U_g\left(x\right)\frac{\partial}{\partial x}\right]^2\left(h_l\right) \quad (17c)$$

$$J_3=-\rho_g h_l^2 A_g\xi\times$$
$$\left[\frac{\partial}{\partial t}+U_g\frac{\partial}{\partial x}-\frac{\partial U_g}{\partial x}-\mu_g\frac{\partial^2}{\partial x^2}\right]\left(\frac{\partial^2}{\partial x^2}U_g\right) \quad (17d)$$

$$\zeta=\frac{1}{2}\left[1+\frac{1}{\pi}\frac{A}{A_g}\sin\left(\frac{\pi h_l}{4R}\right)-\frac{4R}{h_l}+\frac{11A^2}{4\pi h_l^2 A_g}-\frac{2RA}{h_l A_g}\sin\left(\frac{\pi h_l}{4R}\right)^{1.58}\right] \quad (17e)$$

The following approximation is made to express the difference between liquid and gas interfacial pressure terms and end up with one pressure variable:

$$p_{ig}-p_{il}=\sigma\frac{\partial^2 h_l}{\partial x^2} \quad (18)$$

Taitel and Dukler's model[13] is used to calculate the liquid-wall, gas-wall and interfacial shear forces τ.

3 LINEAR STABILITY ANALYSIS

The transient of the system is formulated by Eqs.(1), (2), (16) and (17). Using the general approach presented by Barnea and Taitel[16], operation of linearization generates:

$$\rho_l\frac{\partial U_l}{\partial t}-\rho_g\frac{\partial U_g}{\partial t}+\rho_l U_l\frac{\partial U_l}{\partial x}-\rho_g U_g\frac{\partial U_g}{\partial x}+$$
$$\left(\rho_l-\rho_g\right)g\cos\theta\frac{\partial h_l}{\partial x}-\sigma\frac{\partial h_l}{\partial x^3}+$$
$$\frac{\partial h_l}{\partial x}\left(\rho_l\left[\frac{\partial}{\partial t}+U_l\frac{\partial}{\partial x}\right]^2-\rho_g\left[\frac{\partial}{\partial t}+U_g\frac{\partial}{\partial x}\right]^2\right)\left(h_l\right)-$$
$$\rho_l h_l^2\eta\left[\frac{\partial}{\partial t}+U_l\frac{\partial}{\partial x}-\frac{\partial U_l}{\partial x}-\mu_l\frac{\partial^2}{\partial x^2}\right]\left(\frac{\partial^2}{\partial x^2}U_l\right)+$$
$$\rho_g h_l^2\xi\left[\frac{\partial}{\partial t}+U_g\frac{\partial}{\partial x}-\frac{\partial U_g}{\partial x}-\mu_g\frac{\partial^2}{\partial x^2}\right]\left(\frac{\partial^2}{\partial x^2}U_g\right)=F \quad (19)$$

with

$$F=-\frac{\tau_l S_l}{A_l}+\frac{\tau_g S_g}{A_g}+\tau_i S_i\left(\frac{1}{A_l}+\frac{1}{A_g}\right)-\left(\rho_l-\rho_g\right)g\sin\theta$$

The general approach presented by Barnea[15] is used to obtain dispersion equation. Introducing a linear sinusoidal perturbation into the model:

$$h_l=\bar{h}_l+h_l'\mathrm{e}^{i(\omega t-kx)},\qquad U_l=\bar{U}_l+U_l'\mathrm{e}^{i(\omega t\text{-}kx)},$$
$$U_g=\bar{U}_g+U_g'\mathrm{e}^{i(\omega t\text{-}kx)}$$

the following equations will be obtained from the continuity Eqs.(1) and (2):

$$U_l'=\left[\frac{\omega}{k}-U_l\right]\frac{h_l'}{\bar{H}_l},\quad U_g'=\left[U_g-\frac{\omega}{k}\right]\frac{h_l'}{\bar{H}_g}$$

The source term F is a function of 3 variables (α_l, U_{ls}, U_{gs}), namely,

$$F'=\left(\frac{\partial F}{\partial\alpha_l}\right)_{U_{ls},U_{gs}}\alpha_l+\left(\frac{\partial F}{\partial U_{ls}}\right)_{R_l,U_{gs}}U_{ls}+\left(\frac{\partial F}{\partial U_{gs}}\right)_{R_l,U_{ls}}U_{gs}$$

Substituting the expressions of U_l', U_g' and F' into Eq.(19) gives the following dispersion equation:

$$\left[1+\left(f_l+f_g\right)k^2\right]\omega^2-2\left[ak+\left(f_l\bar{U}_l+f_g\bar{U}_g\right)k^3-i\left(b-\frac{1}{2}\left(f_l\mu_l+f_g\mu_g\right)k^4\right)\right]\omega+$$
$$ck^2-\left[d-\left(f_l\bar{U}_l^2+f_g\bar{U}_g^2\right)\right]k^4-\left[ek-\left(f_l\mu_l\bar{U}_l+f_g\mu_g\bar{U}_g\right)k^5\right]i=0 \quad (20)$$

It can been seen that, if setting $f_l=f_g=0$, Eq.(19) yields the same dispersion equation by adopting the hydrostatic approximation as in Ref.[14].

The neutral stability condition ($\omega_i=0$) is found by letting $\omega=\omega_R+i\omega_i=\omega_R$ in the dispersion equation as follows:

$$2\left[b-\frac{1}{2}\left(f_l\mu_l+f_{\rm g}\mu_{\rm g}\right)k_{\rm c}^4\right]\omega_{\rm R}-$$
$$\left[ek_{\rm c}-\left(f_l\mu_l\bar{U}_l+f_{\rm g}\mu_{\rm g}\bar{U}_{\rm g}\right)k_{\rm c}^5\right]=0 \qquad (21a)$$

$$\left[1+\left(f_l+f_{\rm g}\right)k^2\right]\omega^2-$$
$$2\left[ak+\left(f_l\bar{U}_l+f_{\rm g}\bar{U}_{\rm g}\right)k^3\right]\omega+$$
$$ck^2-\left[d-\left(f_l\bar{U}_l^2+f_{\rm g}\bar{U}_{\rm g}^2\right)\right]k^4=0 \qquad (21b)$$

Hence, the critical wave velocity at the inception of instability is given by

$$C=\frac{\omega}{k}=\frac{e-\left(f_l\mu_l\bar{U}_l+f_{\rm g}\mu_{\rm g}\bar{U}_{\rm g}\right)k_{\rm c}^4}{2b-\left(f_l\mu_l+f_{\rm g}\mu_{\rm g}\right)k_{\rm c}^4} \qquad (22)$$

Substituting Eq.(22) into Eq.(21b) gives the stability criteria:

$$(C-a)^2+\left(c-a^2\right)+$$
$$k_{\rm c}^2\left[f_l\left(C-\bar{U}_l\right)^2+f_{\rm g}\left(C-\bar{U}_{\rm g}\right)^2-d\right]<0 \qquad (23)$$

with

$$a=\frac{1}{\rho}\left[\frac{\rho_l\bar{U}_l^2}{\alpha_l}+\frac{\rho_{\rm g}\bar{U}_{\rm g}}{\alpha_{\rm g}}\right],$$

$$b=\frac{1}{\rho}\left[\left(\frac{\partial F}{\partial U_{{\rm s}l}}\right)_{\alpha_l,U_{\rm sg}}-\left(\frac{\partial F}{\partial U_{\rm sg}}\right)_{\alpha_l,U_{{\rm s}l}}\right],$$

$$c=\frac{1}{\rho}\left[\frac{\rho_l\bar{U}_l^2}{\alpha_l}+\frac{\rho_{\rm g}\bar{U}_{\rm g}^2}{\alpha_{\rm g}}-\left(\rho_l-\rho_{\rm g}\right)\cos\theta\frac{A}{A_l'}\right],$$

$$d=\frac{\sigma}{\rho}\frac{A}{A_l'},\quad e=-\frac{1}{\rho}\left(\frac{\partial F}{\partial\alpha_l}\right)_{U_{{\rm s}l},U_{\rm sg}},\quad f_l=\frac{\rho_l h_l^2\eta}{\rho\alpha_l},$$

$$f_{\rm g}=\frac{\rho_{\rm g}h_l^2\xi}{\rho\alpha_{\rm g}},\quad \rho=\frac{\rho_l}{\alpha_l}+\frac{\rho_{\rm g}}{\alpha_{\rm g}},\quad A_l'={\rm d}A_l/{\rm d}h_l.$$

The stability criteria incorporate the shear stresses, fluid velocities and geometrical relations of the flow, which are in turn functions of the equilibrium liquid holdup. Thus, the first step in implementing this model is to find α_l. The geometrical parameters in two-phase stratified pipe flow are shown in Fig.1. Although the present criterion is given in a general form which includes the shear stresses and does not depend on the particular form of the shear-stress relationship and the friction coefficient, these relationships should be incorporated when practical simulations are sought. In the present calculations the following relations described in Taitel and Dukle[13] are used:

$$\tau_l=\frac{f_l\rho_l U_l^2}{2} \qquad (24a)$$

$$\tau_{\rm g}=\frac{f_{\rm g}\rho_{\rm g}U_{\rm g}^2}{2} \qquad (24b)$$

$$\tau_{\rm i}=\frac{f_{\rm i}\rho_{\rm g}\left(U_{\rm g}-U_l\right)\left|U_{\rm g}-U_l\right|}{2} \qquad (24c)$$

The liquid and the gas friction factors are evaluated from

$$f_l=0.046Re_l^{-0.2} \qquad (25a)$$

$$f_{\rm g}=0.046Re_{\rm g}^{-0.2} \qquad (25b)$$

The critical wave number $k_{\rm c}$ is found numerically. For fixed gas and liquid velocities, with the decreasing of wave number, the value in the right hand side of Eq.(23) increases to a maximum, and then decreases. The critical liquid velocity at the inception of instability is defined as the liquid velocity when the maximum value in the right side of Eq.(23) is zero, and the critical wave number corresponds to the wave number of the “most dangerous wave”. More details can be found in Refs.[15—17].

4 RESULTS AND DISCUSSION

Experiments were carried out in a flow loop facility with an inner diameter of 0.05m and a length of 20m with various inclinations of 0.0°, —0.4°, —0.6°, —0.8° and —1.0° in the State Key Laboratory of Multiphase Flow, Xi’an Jiaotong University. The characteristics of interfacial wave of stratified flow were measured using two-parallel conductance probes. More detailed description of experimental facility, measurement method and data processing is presented in Ref.[20].

Barnea and Taitel[16], Lin and Hanratty[14] developed their models based on a one-dimensional two-fluid model with the hydrostatic approximation. Fig.2 shows the comparison between the experimental and calculated critical liquid height and critical superficial

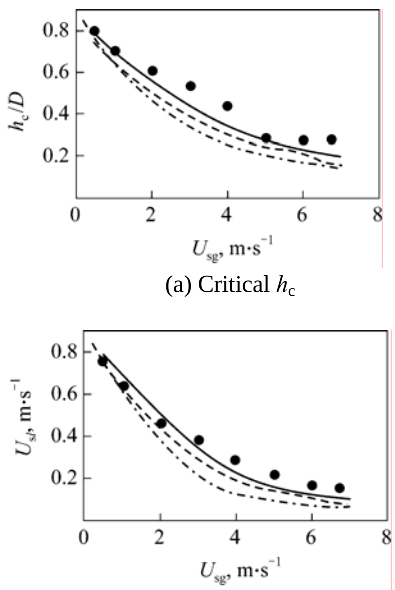

(a) Critical $h_{\rm c}$

(b) Critical U_{sl}

Figure 2 Comparison of neutral stability prediction with experimental data (air-water, D=0.05m, θ=—0.8°)
● exp. data; —— present model; - - - Ref.[16]; -·-· Ref.[14]

liquid velocity, above which the instability of interfacial wave occurs, with a pipe inclination of −0.8°. It can be noted that the predicted values of Barnea and Taitel[16], Lin and Hanratty[14] models are lower than experimental values. The vertical component of phase velocity, especially when superficial gas velocity is high, has great effects on interfacial stability. The prediction of the present model is in best agreement with the experimental data.

Figure 3 depicts the experimental critical liquid height and critical superficial liquid velocity to initiate instability of interfacial wave at different pipe inclinations. The critical liquid height is found to be insensitive to the pipe inclination, especially when the inclination is larger than 0.4°. However, the inclination has a striking effect on critical liquid velocities at low gas velocities. The critical liquid velocities increase sharply due to the effect of gravity as the inclination increases. When the pipe is inclined, the gravity component along flowing direction significantly affects the critical liquid velocity. It is demonstrated that the model presented in this paper can efficiently predict the height of liquid and critical superficial liquid velocities.

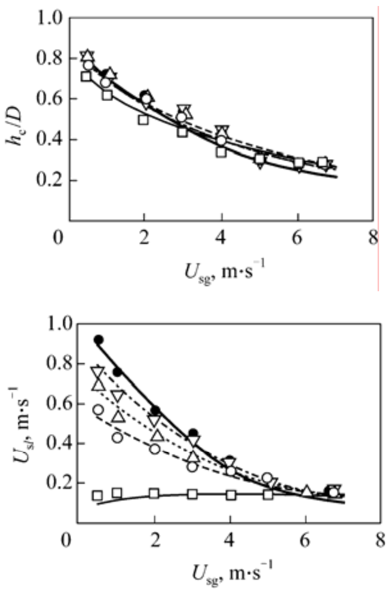

Figure 3 Comparison of neutral stability prediction with experimental data (air-water, D=0.05m)
θ, (°): □ 0 (exp.); ○ −0.4 (exp.); △ −0.6 (exp.); ▽ −0.8 (exp.); ● −1.0(exp.); —— 0 (cal.); - - - −0.4(cal.); ····· −0.6 (cal.); -·-·- −0.8 (cal.); ━━ −1.0 (cal.)

Small pipe inclination has a great effect on interfacial wave velocities when instability of interfacial wave occurs: at a low superficial gas velocity, as the inclination increases, interfacial wave velocity increases; however, when superficial gas velocity is larger than 6.0m·s^{-1}, pipe inclination has little effect on interfacial wave velocity as indicated in Fig.4. There is an excellent agreement between the predicted results and the experimental data.

Andreussi and Bendiksen[21] studied air-water stratified flow in inclined pipes with diameters of 9.53 and 2.52cm. Fig.5 compares Andreussi and Bendiksen observation[21] of the interfacial wave instability to the present model. It shows that the critical liquid height required to initiate instability increases with the increasing of the pipe diameter. Good agreement between theoretical predictions and experimental results is obtained again.

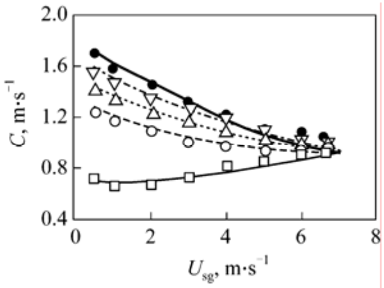

Figure 4 Comparison of interfacial wave velocity prediction with experimental data (air-water, D=0.05m)
θ, (°): □ 0 (exp.); ○ −0.4 (exp.); △ −0.6 (exp.); ▽ −0.8 (exp.); ● −1.0(exp.); —— 0 (cal.); - - - −0.4(cal.); ····· −0.6 (cal.); -·-·- −0.8 (cal.); ━━ −1.0 (cal.)

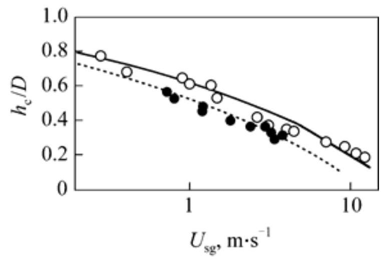

Figure 5 Comparison of neutral stability prediction with results of Ref.[21] (air-water, θ=−1.0°)
D, cm: ○ 9.53 Ref.[21]; —— 9.53(cal.); ● 2.52 Ref.[21]; ····· 2.52 (cal.)

5 CONCLUSIONS

A one-dimensional two-fluid model for stratified flows in a horizontal and nearly horizontal pipe is developed in the current study, in which a more complex closure that included the dynamic pressure terms instead of the hydrostatic approximation, is adopted. A viscous Kelvin-Helmholtz criterion for the prediction of the onset of interfacial wave instability is derived based on the linear analysis of the two-fluid model. The criterion proposed in this paper predicts quantitatively critical conditions required to initiate interfacial wave instability. Both predicted results and experimental data show that critical liquid height is insensitive to small pipe inclinations, while at low gas velocities, critical liquid velocity and critical wave velocity are surprisingly sensitive to small pipe inclinations.

NOMENCLATURE

A	cross-sectional area, m^{-2}
b	local width of cross-section, m
C	wave velocity
D	inside diameter, m
f	friction factor

g	gravitational acceleration, m·s^{-2}
h	film thickness, m
j	superficial velocity, m·s^{-1}
k	wave number, m^{-1}
P	cross-sectional averaged pressure, Pa
p	local pressure, Pa
R	radius, m
S	wetted perimeter, m
t	time, s
U	cross-sectional averaged velocity, m·s^{-1}
u	local velocity, m·s^{-1}
x,y	cartesian coordinate, m
α	phase fraction
θ	pipeline inclination, (°)
μ	viscosity, Pa·s
ρ	density, kg·m^{-3}
σ	surface tension, N·m^{-1}
τ	shear stress, N·m^{-1}
ω	angle velocity, s^{-1}

Subscripts

c	critical value
g	gas phase
i	interfacial
l	liquid phase
s	superficial velocity

REFERENCES

1 Zheng, G., Brill, J.P., "Slug flow behavior in a hilly terrain pipeline", *Int. J. Multiphase Flow*, **20**, 63—79(1994).

2 Bendiksen, K.H., Malnes, D., Nydal, O.J., "On the modeling of slug flow", *Chem. Eng. Commun.*, **141/142**, 71—102(1996).

3 Cook, M., Behnia, M., "Slug length prediction in near horizontal gas-liquid intermittent flow", *Chem. Eng. Sci.*, **55**, 2009—2018(2000).

4 van Hout, R., Barnea, D., Shemer, L., "Evolution of statistical parameters of gas-liquid slug flow along vertical pipes", *Int. J. Multiphase Flow*, **27**, 1579—1602(2001).

5 van Hout, R., Shemer, L., Barnea, D., "Evolution of hydrodynamic and statistical parameters of gas-liquid slug flow along inclined pipes", *Chem. Eng. Sci.*, **58**, 115—133(2003).

6 Taitel, Y., Barnea, D., "Effect of gas compressibility on a slug tracking model", *Chem. Eng. Sci.*, **53**, 2089—2097(1998).

7 Fabre, J., Line, A., "Modeling of two-phase slug flow", *Ann. Rev. Fluid Mech.*, **24**, 21—26(1992).

8 Fan, Z., Lusseyran, F., Hanratty, T.J., "Initiation of slugs in horizontal gas-liquid flows", *AIChE J.*, **39**, 1741—1753(1993).

9 Woods, B.D., Hanratty, T.J., "Influence of Froude number on physical processes determining frequency of slugging in horizontal gas-liquid flows", *Int. J. Multiphase Flow*, **25**, 1195—1223(1999).

10 Milne-Thomson, L.M, Theoretical Hydrodynamics, MacMillan Press, London (1968).

11 Yih, C.S., Fluid Mechanics, McGraw-Hill, New York (1969).

12 Wallis, G.B., Dobson, J.E., "The onset of slugging in horizontal stratified air-water flow", *Int. J. Multiphase Flow*, **1**, 173—193(1973).

13 Taitel, Y., Dukler, A.E., "A model for predicting flow regime transitions in horizontal and near horizontal gas-liquid flow", *AIChE J.*, **22**, 47—55(1976).

14 Lin, P.Y., Hanratty, T.J., "Prediction of the initiation of slugs with linear stability theory", *Int. J. Multiphase Flow*, **12**, 79—98(1986).

15 Barnea, D., "On the effect of viscosity on stability of stratified gas-liquid flow - application to flow pattern transition at various pipe inclinations", *Chem. Eng. Sci.*, **46**, 2123—2131(1991).

16 Barnea, D., Taitel, Y., "Kelvin-Helmholtz stability criteria for stratified flow: Viscous *versus* non-viscous (inviscid) approaches", *Int. J. Multiphase Flow*, **19**, 639—649(1993).

17 Funada, T., Joseph, D.D., "Viscous potential flow analysis of Kelvin-Helmholtz instability in a channel", *Int. J. Multiphase Flow*, **28**, 263—283(2001).

18 Liu, W.S., "Stability of interfacial waves in two-phase flows", In: Proceedings of the 16th Annual Conference of the Canadian Nuclear Society of 1995, Saskatoon, Canada (1995).

19 Barnerjee, S., "Separated flow models (Ⅱ), Higher order dispersion effects in the averaged formulation", *Int. J. Multiphase Flow*, **6**, 241—248(1980).

20 Gu, H.Y., Guo, L.J., "Experimental investigation of slug initiation and evolution in two-phase horizontal flow", In: the 5th International Symposium on Multiphase Flow, Heat Mass Transfer and Energy Conversion, Xi'an, China (2005).

21 Andreussi, P., Bendiksen, K.H., "Investigation of void fraction in liquid slugs for horizontal and inclined gas-liquid pipe flow", *Int. J. Multiphase Flow*, **15**, 937—946(1989).

APPENDIX

The term I_2 in Eq.(12) represents the variation of the transient acceleration term due to the variation in the liquid level. The high order diffusive terms in the expression of $\varphi(x, h_l)$ as well as the $v_l \partial v_l / \partial y$ term, is small compared to $\left[\partial v_l(x, h_l)/\partial t + u_l \partial v_l(x, h_l)/\partial x\right]$, so

$$\varphi(x, h_l) \approx \left(\frac{\partial}{\partial t} + u_l \frac{\partial}{\partial x}\right) v_l(x, h_l) .$$

At the interface with the liquid level h_l, the continuity equation can be expressed as

$$v_l(x, h_l) = \frac{\partial h_l}{\partial t} + u_l(x, h_l)\frac{\partial h_l}{\partial x}$$

for turbulent flow in a pipe, any value between $U(x)$ and $1.2U(x)$ is acceptable for $u_l(x, h_l)$. Using $u_l(x, h_l) = U(x)$, the simplest expression is:

$$\varphi(x, h_l) \approx \left[\frac{\partial}{\partial t} + U_l(x, h_l)\frac{\partial}{\partial x}\right]^2 (h_l)$$

Then it leads to

$$I_2 = \rho_l A_l \frac{\partial h_l}{\partial x}\left[\frac{\partial}{\partial t} + U_l(x, h_l)\frac{\partial}{\partial x}\right]^2 (h_l)$$

The y component of the liquid velocity at the crest is given by

$$v_l(x, h_l) = \frac{\partial h_l}{\partial t} + u_l(x, h_l)\frac{\partial h_l}{\partial x} \approx \frac{\partial h_l}{\partial t} + U_l(x)\frac{\partial h_l}{\partial x}$$

and the global continuity equation for the liquid phase is given by

$$\frac{\partial h_l}{\partial t} + U_l \frac{\partial h_l}{\partial x} = -\frac{A_l}{A_l'}\frac{\partial}{\partial x}U_l$$

and A_l/A_l' can be grossly approximated as h_l, so

$$v_l\left(x,h_l\right)\approx-\frac{A_l}{A_l'}\frac{\partial}{\partial x}U_l\approx-h_l\frac{\partial U_l}{\partial x}$$

while at the bottom of the liquid layer, the velocity profile must fit the condition of $v_l(x,0)=0$, and in the bulk of the liquid layer, the evolution of v_l is governed by

$$\frac{\partial}{\partial y}v_l(x,y)=-\frac{\partial}{\partial x}u_l(x,y)$$

according to the assumption mentioned above: $u(x,y)\approx U_l(x)$. Then an approximation for the local velocity profile within the liquid phase can be expressed as follows:

$$v_l\left(x,y\right)\approx-y\frac{\partial}{\partial x}U\left(x\right)$$

Using the proposed bulk velocity profile: $u(x,y)\approx U_l(x)$ and $v_l(x,y)\approx-y\partial U(x)/\partial x$, the following equation can be obtained:

$$\frac{\partial}{\partial x}\varphi=-y\left[\frac{\partial}{\partial t}+U_l\frac{\partial}{\partial x}-\frac{\partial U_l}{\partial x}-\mu_l\frac{\partial^2}{\partial x^2}\right]\left(\frac{\partial^2}{\partial x^2}U_l\right)$$

by integrating, the term I_3 is obtained:

$$I_3=-\rho_l\chi\left[\frac{\partial}{\partial t}+U_l\frac{\partial}{\partial x}-\frac{\partial U_l}{\partial x}-\mu_l\frac{\partial^2}{\partial x^2}\right]\left(\frac{\partial^2}{\partial x^2}U_l\right)$$

with

$$\chi=\int_0^{h_l}\left(\int_y^{h_l}y'\mathrm{d}y'\right)b\left(y\right)\mathrm{d}y=\frac{1}{2}h_l^2A_l-\frac{1}{2}\int_0^{h_l}y^2b\left(y\right)\mathrm{d}y$$

The integral $\int_0^{h_l}y^2b\left(y\right)\mathrm{d}y$ can be approximated by the explicit expression $h_l^2R^2\sin\left(\pi h_l/4R\right)$. Hence an explicit expression of I_3 is obtained:

$$I_3=-\rho_l h_l^2A_l\eta\left[\frac{\partial}{\partial t}+U_l\frac{\partial}{\partial x}-\frac{\partial U_l}{\partial x}-\mu_l\frac{\partial^2}{\partial x^2}\right]\left(\frac{\partial^2}{\partial x^2}U_l\right)$$

with

$$\eta=\frac{1}{2}\left[1-\frac{1}{\pi}\frac{A}{A_l}\sin\left(\frac{\pi h_l}{4R}\right)\right].$$